PLS-based kinetics modeling and optimization of the oxidative coupling of methane over Na$_2$WO$_4$/Mn/SiO$_2$ catalyst

Mi Ran Lee*, Myung-June Park*,†, Wonjin Jeon**, Jae-Wook Choi**, Young-Woong Suh***, and Dong Jin Suh**

*Department of Chemical Engineering, Ajou University, Suwon 443-749, Korea
**Clean Energy Center, Korea Institute of Science and Technology, Seoul 136-791, Korea
***Department of Chemical Engineering, Hanyang University, Seoul 133-791, Korea

Abstract–Reactor modeling for the oxidative coupling of methane over Na$_2$WO$_4$/Mn/SiO$_2$ catalyst was addressed in the present study. The catalyst loading part was designed to be thicker than the inlet and outlet parts to reduce the rates of side reactions in the gas phase, and the optimal aspect ratio (L to D ratio) for no pressure drop and minimum side reactions was determined in experimental studies. Experiments were also conducted under a variety of operating conditions such as gas hourly space velocity (GHSV), CH$_4$/O$_2$ ratio and reaction temperature, and partial least-squares model was applied to predict the performance of the reactor. The validity of the developed model was corroborated by the comparison with experimental data, and normalized parametric sensitivity analysis was carried out. Finally, the genetic algorithm (GA) was applied to determine the optimal conditions for maximum production of ethane and ethylene.

Key words: Methane, Oxidative Coupling, Partial Least Squares, Mathematical Modeling, Optimization, Na$_2$WO$_4$/Mn/SiO$_2$ Catalyst

INTRODUCTION

The large reserves of natural gas can serve as one of the alternative energy sources and as the feedstock for the production of chemicals. Among several methane conversion processes such as Fischer-Tropsch synthesis and methanol synthesis, oxidative coupling of methane (OCM) is getting a focus since it obviates the utilization of intermediate steps like a reforming process and produces valuable products in a direct manner. However, the yield of C$_2$ hydrocarbons never exceeds a limit between 22% and 27% [1,2], which motivates the research on the development of high performance catalysts.

A large number of catalysts, such as alkali-promoted alkaline earth metal oxides, transition metal oxides and rare earth metal oxides, have been found to show good activity and selectivity in the OCM reaction [3-5]. The Na$_2$WO$_4$/Mn/SiO$_2$ catalyst, first reported by Fang et al. [6], is one of the most effective catalysts. Ji and coworkers suggested that the active sites of Na$_2$WO$_4$/Mn/SiO$_2$ gel catalysts are WO$_4$, and the reason for high CH$_4$ conversion and C$_2$ selectivity may lie in the fact that WO$_4$ has suitable geometric and energy-matching properties to extract hydrogen of CH$_4$ [7].

Kinetic modeling studies are useful in the interpretation and optimization of laboratory data concerning the importance of homogeneous and heterogeneous reactions. Furthermore, the results of kinetic modeling can be used to predict the role of different operating variables and save time required for the experimental work. Since the OCM is a complex reaction network of parallel and consecutive, heterogeneous as well as homogeneous reaction steps, numerous reaction models have been presented to describe the performance of the OCM process. Stansch et al. [8] developed an overall kinetic model composed of nine heterogeneous reactions and one homo-geneous reaction for La$_2$O$_3$/CaO catalyst, and Shahri et al. [9] applied Stansch et al.'s model to compare simulation results with experimental data for Na$_2$WO$_4$/Mn/SiO$_2$ catalyst. Sun et al. [10] proposed a model with 39 elementary steps of gas-phase reactions and 14 catalytic reactions over Li/MgO and Sn/Li/MgO, and they compared sensitivities of two catalysts. However, mechanistic models on the basis of detailed kinetics suffer from problems with high computational and time loading, and thus, chemometrics-based models have been suggested as an alternative to overcome problems of first-principles models [11]. Among the methods based on chemometrics, the partial least squares (PLS) [12] model has been most popularly used because it deals with the problems of collinearity and the high dimension of data blocks. Standard linear PLS involves the projection of X, which relates to the process variables (inputs), and Y, which corresponds to the quality or reference variables (outputs), onto a subset of latent variables that are referred to as the input and output scores. As discussed by Baffi et al. [13] when applying linear PLS to a nonlinear problem, the minor latent variables cannot necessarily be discarded because they may describe not only the noise in the data but also significant components of the variance-covariance structure.

In the present study, PLS-based modeling approach was applied to predict the effect of gas hourly space velocity (GHSV), CH$_4$/O$_2$ ratio and temperature on CH$_4$ conversion and C$_2$ yield. Experiments were conducted using a specially designed reactor to minimize the contribution of side reactions, and the data under a variety of conditions were used to construct an empirical model using partial least squares method.

EXPERIMENTAL SECTION

1. Catalyst Preparation

The Na$_2$WO$_4$/Mn/SiO$_2$ gel catalyst was used in this work since it has been reported as one of the efficient catalysts for the oxida-

tive coupling of methane [6,14]. The catalyst was prepared by an incipient wetness impregnation method [15]. A silica gel support (Sigma-Aldrich, Davisil 636, 35-60 mesh) was first impregnated with an aqueous solution of $Mn(NO_3)_2 \cdot 6H_2O$ (Kanto Chemical Co., Inc.) and dried at 105 °C for 6 h, and then an aqueous solution of $Na_2WO_4 \cdot 2H_2O$ (JUNSEI) was introduced to the Mn-impregnated samples. The resulting samples were dried at 105 °C for 6 h and finally calcined in air at 800 °C for 5 h. The prepared catalysts were sieved to 40-60 mesh to prevent the pressure drop in a reactor.

2. Reactor Design

To prevent a pressure drop, the catalytic loading part was designed to be thicker than the inlet and outlet parts, as shown in Fig. 1. In the first step, different inner diameters (ID_{narrow}) for the inlet and outlet parts were tested with quartz chips packed in the tube, and no pressure drop was observed for the diameter higher than 4 mm. As for the thicker part: different inner diameters (ID_{wide}) of 7 and 10 mm with the ratio of L_{wide}/ID_{wide} fixed at 4 and ID_{narrow} specified as 4 mm. Inner diameter of 7 mm showed the pressure drop of *ca.* 0.7%, while ID_{wide} of 10 mm had no pressure drop. Fig. 2 shows the methane conversion and the C_2 yield when the mixture of CH_4 and O_2 ($CH_4/O_2=5$) flowed through the reactor ($ID_{narrow}=4$ mm, $ID_{wide}=$
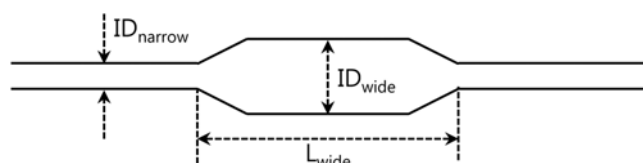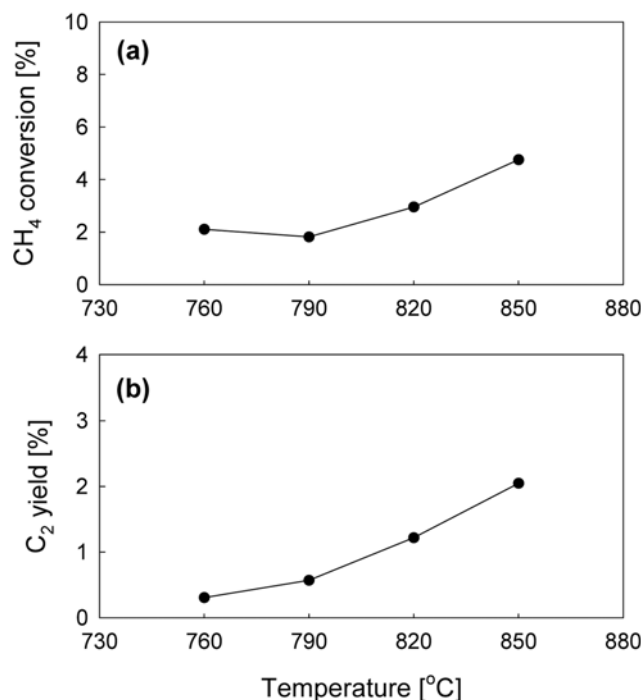

Fig. 1. Detailed structure of the reactor.

Fig. 2. Blank test of the reactor under different reaction temperatures. (a) CH_4 conversion and (b) C_2 yield when the ratio of $CH_4/O_2=5$, $ID_{narrow}=4$ mm, $ID_{wide}=10$ mm, $L_{wide}=40$ mm, GHSV=10,000 h^{-1} with no catalysts loaded in the reactor.
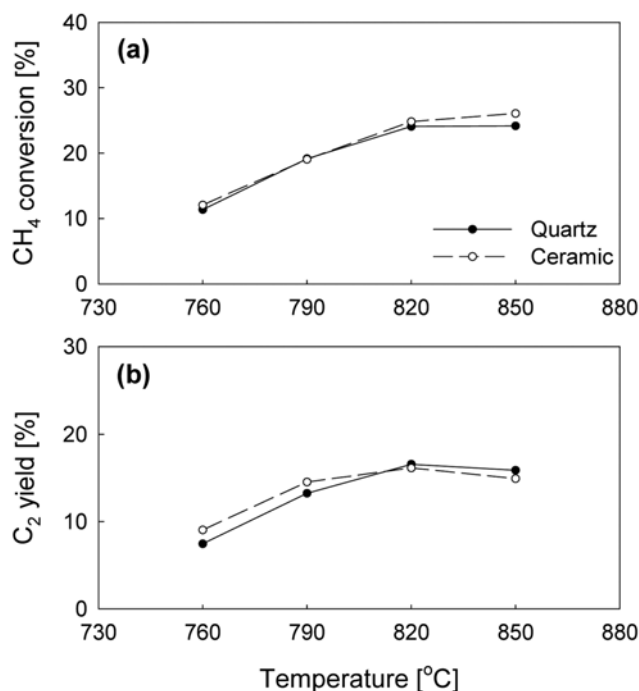

Fig. 3. The effects of the type of packing materials when the reactor is loaded with catalysts. (a) CH_4 conversion and (b) C_2 yield when the ratio of $CH_4/O_2=5$, $ID_{narrow}=4$ mm, $ID_{wide}=10$ mm, $L_{wide}=40$ mm, GHSV=10,000 h^{-1}.

10 mm, $L_{wide}=40$ mm) at the GHSV of 10,000 h^{-1} with no catalysts loaded in the reactor. For all the reaction temperatures, the methane conversions and the C_2 yields were maintained below 5% and 2%, respectively, and it is inferred from the results that the reactor specification is effective for the least side reactions and no pressure drop.

Secondly, the effects of different packing materials were compared, and the results with catalyst loaded in the thicker part are provided in Fig. 3. There was little effect of quartz chips and ceramic beads on the methane conversion and C_2 yield, but quartz chips had difficulty in consistency due to their non-uniform shape. Therefore, ceramic beads were used in this work.

3. Reaction Procedure

The catalytic reaction was performed in a reactor system depicted in Fig. 4. The inner diameter for the inlet and outlet of the reactor is 4 mm and the thicker part has a 10 mm of inner diameter. The catalyst was packed in the middle of the reactor. The rest space of the reactor was packed with inert ZrO_2-SiO_2 (Cenotec Co. LTD.) beads to preheat the reactants in the prior catalytic region and minimize homogeneous side reactions in the post catalytic region. A K-type thermocouple was attached to the outside wall of the reactor to control and monitor reaction temperature.

The reactants, CH_4 (99.97%), O_2 (99.5%) and N_2 (99.99%), were co-fed into the reactor through a pre-mixing unit. A cold trap immersed into a chiller (JEIO TECH, VTRC-620) was connected to the exit of the reactor for separating any liquid product from the product stream. The gaseous products were analyzed with on-line gas chromatography (Agilent 7890A) equipped with FID and TCD. H_2, O_2, N_2, CO, and CO_2 were detected by TCD with a column packed with the 60/80 Carboxen-1000 while C_1-C_3 hydrocarbons were analyzed by FID with the Carboxen 1006 PLOT column.
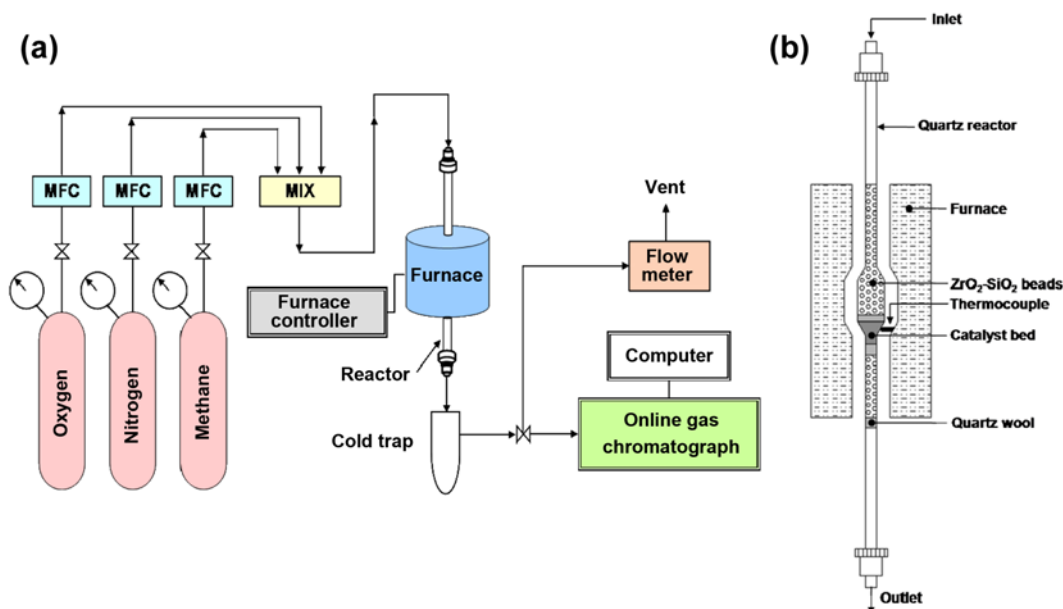
Fig. 4. Schematic diagram of (a) the reaction system and (b) the reactor inside the furnace.

Prior to the catalytic activity test, the catalyst was pretreated at 700 °C under N_2 flow for 1 h and experiments were performed in a temperature range of 760-850 °C with varying the CH_4/O_2 ratio from 2 to 8 and gas hourly space velocity (GHSV) from 5,000 to 30,000 h^{-1}. In all experiments, the catalytic activity was evaluated by conversion, selectivity and yield. The conversion, selectivity and yield were defined as follows:

$$\text{Methane conversion [\%]} = \frac{\text{moles of } CH_4 \text{ converted}}{\text{moles of } CH_4 \text{ in feed}} \times 100 \quad (1)$$

Selectivity of ethane/ethylene [%]

$$= \frac{2 \times (\text{moles of ethane/ethylene})}{\text{moles of } CH_4 \text{converted}} \times 100 \quad (2)$$

Yield of product i [%]

$$= \frac{(\text{methane conversion}) \times (\text{selectivity of i})}{100} \quad (3)$$

Here, selectivities of CO and CO_2 are calculated by replacing the numerator of Eq. (2) with (moles of CO or CO_2).

Since the properties in Eqs. (1) to (3) are strongly dependent on the operating conditions and the effects of those parameters are severely correlated with each other, it is important to develop a quantitative model to predict the effect of experimental conditions and determine the optimal operating strategies. In the subsequent section, brief theories on the partial least squares (PLS) model, which is one of the most widely used statistical models due to its efficiency, are introduced, and then the PLS method is applied to develop a model for the OCM reactions.

RESULTS AND DISCUSSIONS

1. Partial Least Squares Model

A general method for construction of a model with the relationship Y=f(X) is multiple linear regression (MLR) [12]. This can be represented mathematically as

$$Y=XB+E_{MLR} \quad (4)$$

where **X**, **Y**, **B** and $\mathbf{E}_{MLR}$ represent the regressor (or input) block, the response (or output) block, the regression (or sensitivity) matrix and the residual matrix, respectively. When the number of independent variables (m) is lower than the number of samples (n), there is no exact solution, but an approximate solution can be determined by minimizing the magnitude of the residual vector ($\mathbf{E}_{MLR}$). The least squares solution is given by

$$\mathbf{B}=(\mathbf{X}^T\mathbf{X})^{-1}\mathbf{X}^T\mathbf{Y} \quad (5)$$

This equation reveals a common problem in MLR, namely, the inverse of $\mathbf{X}^T\mathbf{X}$ may be difficult to compute if the input data block is high dimension and its elements are highly correlated, which is denoted collinearity or singularity. The PLS approach provides an alternative to overcome this problem.

PLS methods involve an approximation of the **X** and **Y** spaces with their respective score matrices and the maximization of the correlation between the original data blocks [11,12]. A simplified model consists of a regression between the scores for the **X** and **Y** blocks. The PLS model can be interpreted as consisting of outer relations (**X** and **Y** blocks individually) and an inner relation (linking both blocks). The outer relations for the **X** and **Y** blocks are

$$\mathbf{X} = \mathbf{TP}^T + \mathbf{E} = \sum_{h=1}^{N_{LV}} \mathbf{t}_h \mathbf{p}_h^T + \mathbf{E} \quad (6)$$

$$\mathbf{Y} = \mathbf{UQ}^T + \mathbf{F}^* = \sum_{h=1}^{N_{LV}} \mathbf{u}_h \mathbf{r}_h^T + \mathbf{F}^* \quad (7)$$

Each pair of latent variables accounts for a certain amount of the variability in the input and output blocks. The first N_{LV} latent variables account for most of the variance of the data blocks, and the other latent variables capture measurement and/or process noise in the data. It is the intention to both describe **Y** accurately (make $\|\mathbf{F}^*\|$) and, at the same time, construct an efficient representation between **X** and **Y**. A simple criterion for model building is to use a thresh-

Table 1. Experimental conditions[a]

Parameters	Values	Units
GHSV	5,000/7,000/10,000/15,000/20,000/30,000	h^{-1}
CH_4/O_2 ratio	2/3.5/5/6.5/8	-
Temperature	760/790/820/850	^{o}C

[a]Conditions were determined in a full-factorial manner, and thus, total number of conditions is 120 ($6 \times 5 \times 4$)

old value for F^*, but cross validation can be used to determine the number of latent variables for a robust model [13].

The simplest model for the inner relation is a linear one:

$$\hat{\mathbf{u}}_h = b_h \mathbf{t}_h \quad (8)$$

where $b_h = \hat{\mathbf{u}}_h \mathbf{t}_h / \mathbf{t}_h^T \mathbf{t}_h$ plays the role of the regression coefficient in the multiple linear regression (MLR) and the principal component regression (PCR) model. Finally, the prediction model for quality variables is constructed applying the PLS algorithm in linear regression form as follows [16]:

$$\hat{\mathbf{y}}_h = \mathbf{x}^T \hat{\mathbf{b}} \quad (9)$$

2. Mathematical Modeling

To obtain kinetic data for mathematical modeling, GHSV (x_1), CH_4/O_2 ratio (x_2) and temperature (x_3) were specified as manipulated variables, and experimental conditions were determined to be a total of 120 conditions on the basis of full-factorial (cf. Table 1). In addition, nonlinear terms are included in the input vector to address the nonlinearity of the relationship as follows:

$$\mathbf{x}^T = [x_1, x_2, x_3, x_1^2, x_2^2, x_3^2, x_1^{-1}, x_2^{-1}, x_3^{-1},$$
$$\sqrt{x_1}, \sqrt{x_2}, \sqrt{x_3}, x_1 x_2, x_2 x_3, x_3 x_2] \quad (10)$$

Since the number of experimental conditions is 120, the input data block ($\mathbf{X}$) is 120×15 matrix, while the output data block ($\mathbf{Y}$) is composed of 10 properties including CH_4 and O_2 conversions, selectivities of ethylene, ethane, CO and CO_2 under the corresponding experimental conditions.

The input and output data blocks were scaled to prevent ill-conditioning problem resulting from different magnitudes of orders between variables in such a way that all the variables have mean and variance of 0 and 1, respectively. PLS modeling showed the first three latent variables cover more than 96% variances of the input block, while at least nine latent variables are necessary to capture more than 80% of the output data block. However, as discussed by Baffi et al. [13], when applying linear PLS to a nonlinear problem, the minor latent variables cannot necessarily be discarded because they may describe not only the noise in the data but also significant components of the variance-covariance structure. In addition, the calculation with different number of latent variables showed that a total of 15 latent variables should be used for the best performance of the PLS model. Fig. 5 shows the comparison between experimental data and simulation results, and it is clearly shown that the performance of the PLS-based model is satisfactory.

3. Sensitivity Analysis and Optimization

The developed PLS-model can be used to evaluate the effect of operating conditions. Normalized parametric sensitivity is defined as the ratio of the fractional change of the output to the fractional change of the parameter, that is, ($\Delta y/y$) divided by ($\Delta p/p$). In the
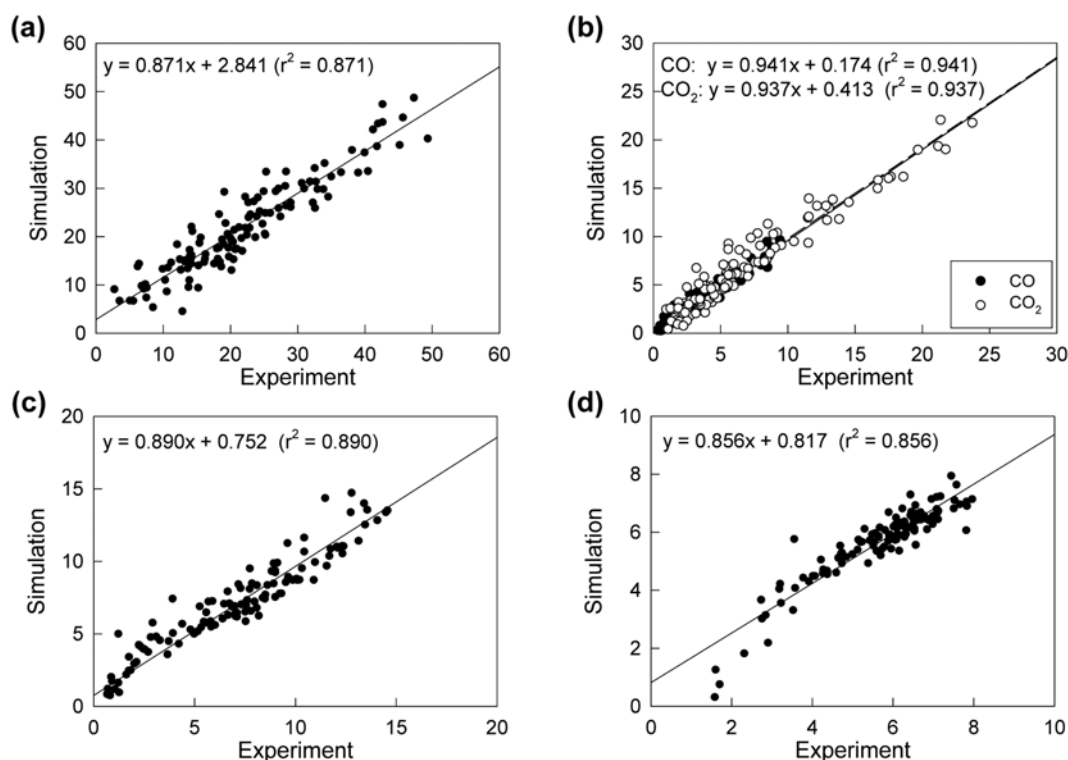

Fig. 5. Comparison of (a) CH_4 conversion, (b) CO and CO_2 yield, (c) ethylene yield and (d) ethane yield between experimental data and simulation results.
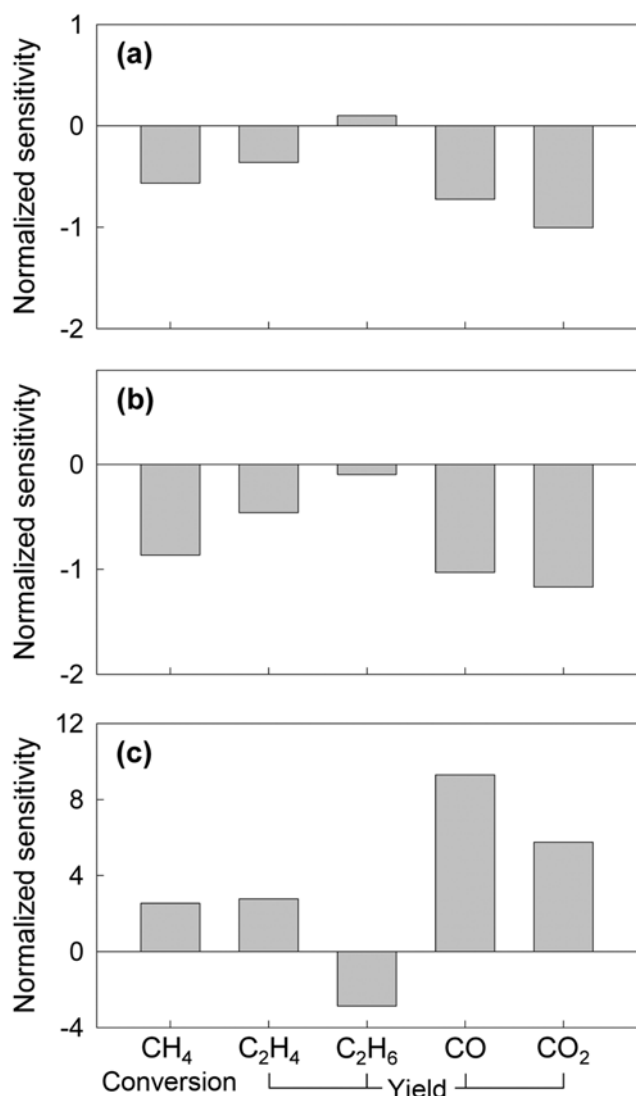
Fig. 6. Normalized sensitivity of CH₄ conversion, ethylene yield, ethane yield, CO yield and CO₂ yield with respect to (a) GHSV, (b) CH₄/O₂ ratio and (c) reaction temperature.

much more than the C_2 products, which may lead to higher selectivity for ethylene and ethane. This result implies that high GHSV may be preferred for low side reaction rates. Increased CH_4/O_2 ratio results in the decreased CH_4 conversion (cf. Fig. 6(b)), and the values for yields are also decreased. However, the reduced amount of oxygen leads to lower reaction rates for CO and CO_2 production, and thus, the sensitivity values for those species are much lower than ethylene and ethane. As shown in Fig. 6(c), the effect of reaction temperature is dominant compared to the other parameters. High temperature is beneficial for CH_4 conversion and ethylene yield at the expense of ethane yield, and the production of more CO and CO_2 is also problematic.

In spite of sensitivity analysis, parameters and outputs are highly correlated, and thus it is difficult to determine the optimal conditions for the oxidative coupling of methane. Therefore, genetic algorithm was applied, where the developed PLS-model was used and the ranges of parameters in Table 1 were specified as constraints, since the empirical model such as PLS-model is usually effective within the range of its development. Optimization was conducted for two objectives: maximum C_2 selectivity (Case 1) and maximum C_2 yield (Case 2). For both optimizations, the optimal values for input parameters were almost the same (cf. Table 2), which means that high GHSV and high temperature with CH_4/O_2 ratio fixed at 2.2 produces maximum amount of C_2 products. The resulting C_2 yield of 27.2% is higher than the reported values for maximum production [1,2]. However, when the calculated conditions are implemented in the actual process, the C_2 yield might be lower than the expected value, attributable to the model mismatch and other types of disturbances such as measurement errors. If additional experimental data under different conditions from those in the present work are included in the PLS model, the model mismatch might be reduced to improve the performance of the model prediction and to prove the validity of the calculated optimal operating conditions.

CONCLUSIONS

In a specially designed reactor to minimize the effect of side reactions in the oxidative coupling of methane (OCM), experiments were conducted under various conditions with GHSV, CH_4/O_2 ratio and reaction temperature as manipulated variables, and the partial least squares (PLS) model was developed for the purpose of quantitative analysis of the reaction. The comparison between experimental data and simulation results validated the effectiveness of the developed model, and normalized parametric sensitivity clearly showed the effect of operating conditions. Finally, the optimal operating condition was also determined using the genetic algorithm, guaranteeing the maximum yield of C_2 products. Therefore, the reactor design and PLS-model based approach in this work can be extended to the development of efficient OCM processes.

present study, outputs are specified as the CH_4 conversion and the yields of C_2H_4, C_2H_6, CO and CO_2, while the parameters are selected with GHSV, CH_4/O_2 ratio in the feed and reaction temperature. As for the effect of GHSV, Fig. 6(a) shows negative effects on the outputs except ethane yield. This feature is attributed to the fact that the ethane is produced in the gas phase and then, it is re-adsorbed on the catalyst surface to produce ethylene product [17]. In other words, the decreased residence time by the increased GHSV produces more ethane than ethylene. In addition, CO and CO_2 yields are reduced by the increased GHSV and the degree of reduction is

Table 2. Optimal operating conditions by the genetic algorithm (GA)

	Input			CH₄ conversion [%]	Selectivity [%]			Yield [%]		
	GHSV [h⁻¹]	CH₄/O₂ ratio	Temp. [°C]		C₂H₄	C₂H₆	C₂	C₂H₄	C₂H₆	C₂
Case 1	23,385	2.2	850	36.1	40.1	35.0	75.1	14.5	12.6	27.1
Case 2	21,506	2.2	850	34.8	41.2	36.9	78.2	14.3	12.8	27.2

ACKNOWLEDGEMENTS

REFERENCES

1. L. Mleczko and M. Baerns, *Fuel Process. Technol.*, **42**, 217 (1995).
2. Y. S. Su, J. Y. Ying and W. H. Green, *J. Catal.*, **218**, 321 (2003).
3. A. G. Dedov, A. S. Loktev, I. I. Moiseev, A. Aboukais, J.-F. Lamonier and I. N. Filimonov *Appl. Catal. A: Gen.*, **245**, 209 (2003).
4. D. Papageorgiou, A. M. Efstathiou and X. E. Verykios, *Appl. Catal. A: Gen.*, **111**, 41 (1994).
5. N. G. Maksimov, G. E. Selyutin, A. G. Anshits, E. V. Kondratenko and V. G. Roguleva, *Catal. Today*, **42**, 279 (1998).
6. Z. C. Jiang, C. J. Yu, X. P. Fang, S. B. Li and H. L. Wang, *J. Phys. Chem.*, **97**, 12870 (1993).
7. S. Ji, T. Xiao, S. Li, L. Chou, B. Zhang, C. Xu, R. Hou, A. P. E. York and M. L. H. Green, *J. Catal.*, **220**, 47 (2003).
8. Z. Stansch, L. Mleczko and M. Baerns, *Ind. Eng. Chem. Res.*, **36**, 2568 (1997).
9. S. M. K. Shahri and S. M. Alavi, *J. Nat. Gas Chem.*, **18**, 25 (2009).
10. J. Sun, J. W. Thybaut and G. B. Marin, *Catal. Today*, **137**, 90 (2008).
11. M. A. Sharaf, D. L. Illman and B. R. Kowalski, *Chemometrics*, John Wiley & Sons, New York (1986).
12. P. Geladi and B. R. Kowalski, *Anal. Chim. Acta*, **185**, 1 (1986).
13. G. Baffi, E. B. Martin and A. J. Morris, *Comput. Chem. Eng.*, **23**, 395 (1999).
14. J. H. Lunsford, *Angew. Chem. Int. Ed.*, **34**, 970 (1995).
15. S. Pak, P. Qiu and J. H. Lunsford, *J. Catal.*, **179**(1), 222 (1998).
16. M.-J. Park, M. T. Dokucu and F. J. Doyle III, *Ind. Eng. Chem. Res.*, **43**, 7227 (2004).
17. J. S. Ahari, R. Ahmadi, H. Mikami, K. Inazu, S. Zarrinpashne, S. Suzuki and K.-I. Aika, *Catal. Today*, **145**, 45 (2009).